Supporting Information

for

Solution-air interface synthesis and growth mechanism of tooth enamel-like hydroxyapatite/chondroitin sulfate films

Yifei Xu, Guobin Ma,* Xiyan Wang, and Mu Wang*

National Laboratory of Solid State Microstructures, and Department of Physics, Nanjing University, Nanjing 210093, China

I. Distinguishing the S- and A-faces

We performed the following experiments to distinguish the "A-face" and the "S-face". When growing samples were visible at the air-solution interface, we collected some on copper grids (100 mesh parallel bar) and examined the samples by a scanning electron microscope (LEO 1530VP FESEM). Two ways were taken to collect the samples. One was to carefully insert a grid beneath a sample and slowly lift it up from the solution. After successive treatment, the morphology of the sample was examined by SEM, which represented the "air-face" of the film. The other was to carefully place a grid on top of the sample to "stick" it. The grid was then lifted up and turned over with caution, and the observed morphology of the sample represented the "solution-face". As shown in Figure S1, the "A-face" is fairly flat but the "S-face" contains "domes".

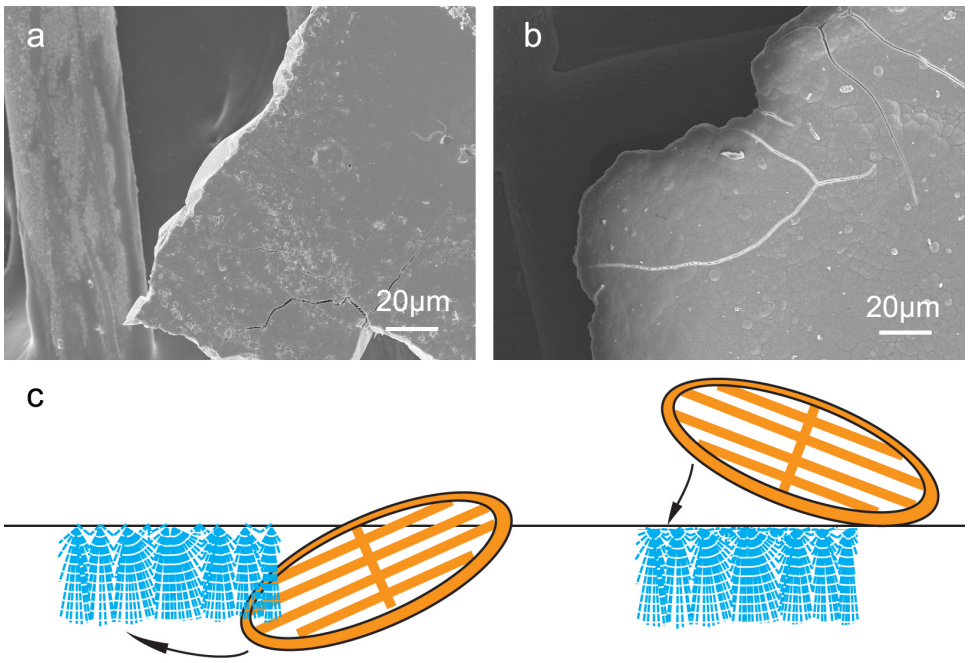

Figure S1. (a), (b) SEM images for samples collected on copper grids by ways illustrated in (c), respectively. One can see that the "A-face" in (a) is flat, whereas the "S-face" in (b) contains "domes".

II. XRD spectra analysis

XRD spectra shown in Figure 3a were analyzed by way of Gaussian fits of the diffraction peaks. Note that I_{002}/I_{211} and $I_{002}/I_{211,112,300}$ for HAP or FAP powders is ~37% and ~15%, respectively.

Table S1. FWHMs of (002) XRD diffraction peaks, I_{002}/I_{211}, and $I_{002}/I_{211,112,300}$ for the samples prepared with 0, 0.1, and 1.0 mM F^-, respectively.

	Batch #1 with F^- of			Batch #2 with F^- of		
	0 mM	0.1 mM	1.0 mM	0 mM	0.1 mM	1.0 mM
$FWHM_{002}$	0.35	0.25	0.19	0.29	0.24	0.18
I_{002}/I_{211}	0.84	0.56	2.07	0.65	0.83	1.53
$I_{002}/I_{211,112,300}$	0.61	0.36	0.93	0.43	0.68	1.10

III. Zeta potential measurements

HAP nanocrystals with and without ChS were prepared respectively. HAP nanocrystals with ChS (denoted hereafter as HAP/ChS) were synthesized using the non-evaporation method described in this manuscript. The ChS concentration was 2.0 g/L, and the initial pH was 5.0. Pure HAP nanocrystals were synthesized at pH of 12.0 by the method we have reported.[1] SEM and XRD results for the samples are shown in Figure S2.

HAP/ChS and pure HAP nanocrystals were thoroughly centrifuge washed by de-ionized water and then washed by 150 mM NaCl solution with pH of 6.0. After drying, 50 mg of each powder was suspended respectively in 100 mL of 150 mM NaCl solutions with ChS concentrations of 0, 0.01, 0.05, 0.1, 1.0, and 5.0 g/L. The suspensions were then supersonically treated and their zeta potentials were measured. All the measurements were performed at 25 °C, and the pHs of the solutions were adjusted to 6.0. ChS and Ca^{2+} solutions contain 2.0 g/L ChS and 0, 1.0, 10.0, and 50.0 mM Ca^{2+}, respectively.

Table S2. Measured zeta potentials for HAP/ChS crystals and HAP nanocrystals suspended in solutions with different ChS concentrations. The mobilities and conductivities are also listed.

ChS (g/L)	HAP/ChS Crystals			HAP Crystals		
	Zeta potential (mV)	Mobility (μm·cm/Vs)	Conductivity (mS/cm)	Zeta potential (mV)	Mobility (μm·cm/Vs)	Conductivity (mS/cm)
0	-21.81±0.17	-1.71±0.01	12.21±0.24	-3.64±0.42	-0.28±0.03	13.0±0.54
0.01	-21.20±0.80	-1.66±0.06	12.01±0.24	-8.15±0.21	-0.64±0.02	12.4±0.46
0.05	-22.15±0.98	-1.73±0.08	12.34±0.25	-18.7±1.04	-1.47±0.08	12.6±0.33
0.1	-20.31±0.12	-1.59±0.01	11.97±0.29	-22.3±0.43	-1.75±0.03	12.6±0.29
1.0	-23.24±0.34	-1.81±0.03	12.63±0.25	-24.5±0.29	-1.92±0.02	12.4±0.33
5.0	-21.82±1.36	-1.71±0.11	12.67±0.29	-24.2±0.43	-1.90±0.03	12.6±0.33

Table S3. Measured zeta potentials for solutions with 2.0 g/L ChS and different concentrations of Ca^{2+}. The mobilities and conductivities are also listed.

Concentration of Ca^{2+} (mM)	Zeta potential (mV)	Mobility (μm·cm/Vs)	Conductivity (mS/cm)
0	-23.06±2.35	-1.81±0.15	0.42±0.01
1	-22.87±1.88	-1.79±0.18	0.52±0.01
10	-12.96±0.61	-1.02±0.05	2.65±0.18
50	-7.79±0.72	-0.61±0.06	10.05±0.31

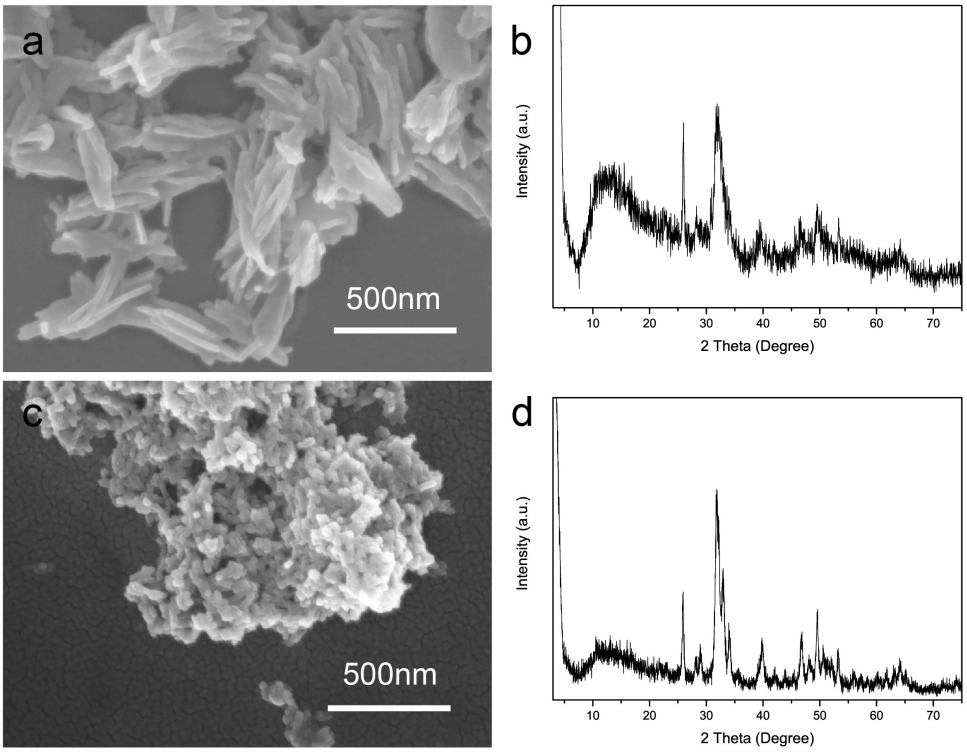

Figure S2. (a) SEM image and (b) XRD pattern for HAP/ChS crystals. (c) SEM image and (d) XRD pattern for HAP nanocrystals.

IV. Mechanical properties

Microindentation analysis was performed on an MTS-XP mechanical testing system using a diamond conical indenter with a tip radius of 10 μm.

The elastic modulus (*E*) and hardness (*H*) are on the order of 10 GPa and 0.5 GPa, respectively (Table S4). The values are several times smaller that those of mature human tooth enamel.[2] Mechanical properties of inorganic/organic composites are influenced by various factors, such as the ratio of the mineral and organics, crystal size and morphology, and the hierarchical structures.[3] More organics (~6%) in our products comparing to those in enamel (~0.1%) could be the main reason for the smaller elastic modulus and hardness.[4]

Another possible reason could be related to measurement error. In our experiments,

indentation was measured on the S-face, since the structures of the S-face closely represent the tooth enamel. As demonstrated in the manuscript, the S-faces of our samples are made up of "domes" whose size increases with F^-. Because the mechanical properties of the tested materials are calculated on the assumption that the sample surface is flat, surface roughness has a strong effect on the dispersion of results in instrumented indentation testing.[5]

We used a conical indenter with radius of 10 μm and set the indentation depth to 1 μm for the measurement. The corresponding diameter of the ideal indentation is 8.7 μm. SEM observations give rise to much smaller values, especially for the 1.0 mM F^- sample. The diameters of the 0 mM, 0.1 mM, and 1.0 mM F^- samples are in the range of ~3–7.5 μm, ~1.5–3 μm, and ~1–2 μm, respectively.

Table S4. The microindentation results of the samples grown with different concentrations of F^-. The data of tooth enamel and dentin are also presented for comparison.

	F^- concentration (mM)			Enamel[a]	Dentin[b]
	0	0.1	1.0		
E (GPa)	17.53±2.24	13.26±3.23	8.93±2.87	80.35±7.71	11.59±3.95
H (GPa)	0.55±0.05	0.51±0.20	0.25±0.09	4.88±0.35	0.52±0.24

[a] Data tested by Xu et al.[2]
[b] Data tested by Mahoney et al.[6]

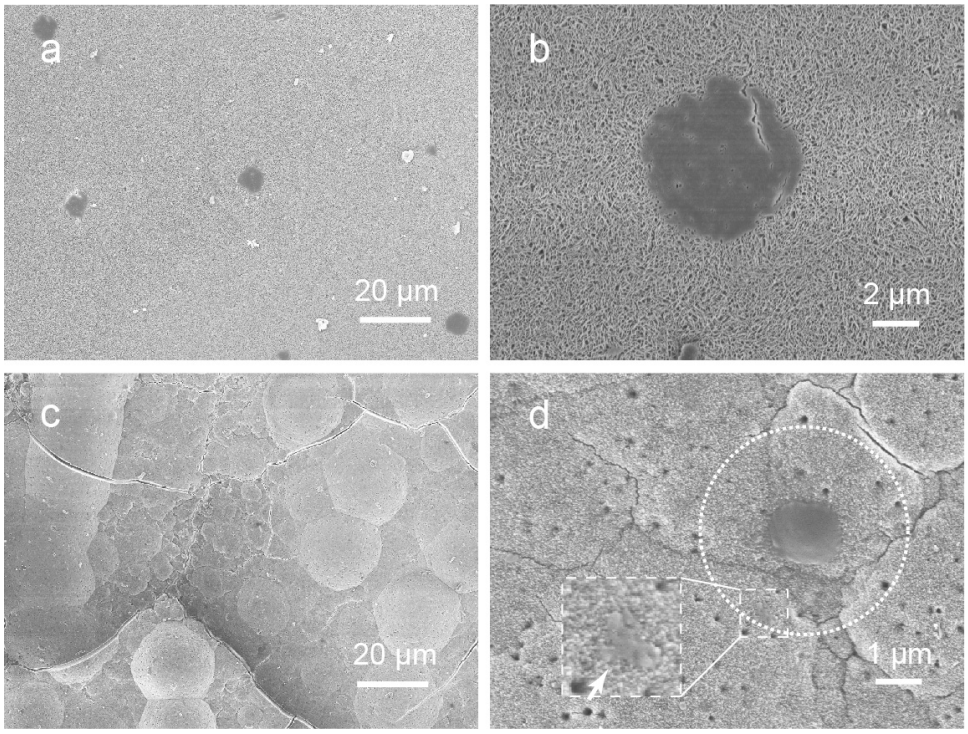

Figure S3. (a), (b) SEM images of the surface morphology and typical indentation of the 0 mM F^- sample, respectively. (c), (d) SEM image of the surface morphology and typical indentation of the 1.0 mM F^- sample, respectively. A typical damaged area close to the indentation pit is arrowed in (d),

Figure S3 shows the morphologies and typical indentations of the 0 mM and 1.0 mM F^- samples. One can see that the 1.0 mM F^- sample has a rougher surface and smaller indentation diameter. However, we noticed that areas characteristic of indentation were frequently found near the indentation pits in the 0.1 mM and 1.0 mM F^- samples. For example, the arrowed area in Figure S3d. If we draw a circle as in Figure S3d, it comes out that the diameter of this circle is ~4.5 μm. The fact indicates that surface roughness has intense influence on the accuracy of the mechanical results. We therefore believe that smaller elastic moduli of the 0.1 and 1.0 mM F^- samples are due to surface roughness related measurement error.[5]

References

1. Ma, G. B.; Liu, X. Y., Hydroxyapatite: Hexagonal or Monoclinic? *Crystal Growth & Design* **2009,** *9* (7), 2991-2994.

2. Xu, H. H. K.; Smith, D. T.; Jahanmir, S.; Romberg, E.; Kelly, J. R.; Thompson, V. P.; Rekow, E. D., Indentation damage and mechanical properties of human enamel and dentin. *Journal of Dental Research* **1998,** *77* (3), 472-480.

3. (a) Gao, H. J.; Ji, B. H.; Jager, I. L.; Arzt, E.; Fratzl, P., Materials become insensitive to flaws at nanoscale: Lessons from nature. *Proc. Natl. Acad. Sci. U. S. A.* **2003,** *100* (10), 5597-5600; (b) Kamat, S.; Su, X.; Ballarini, R.; Heuer, A. H., Structural basis for the fracture toughness of the shell of the conch Strombus gigas. *Nature* **2000,** *405* (6790), 1036-1040; (c) D. Hull, T. W. C., *An Introduction to Composite Materials*. 2nd Edition ed.; Cambridge Univ. Press: Cambridge, UK, 1996

4. Palmer, L. C.; Newcomb, C. J.; Kaltz, S. R.; Spoerke, E. D.; Stupp, S. I., Biomimetic Systems for Hydroxyapatite Mineralization Inspired By Bone and Enamel. *Chem. Rev.* **2008,** *108* (11), 4754-4783.

5. (a) Conte, N., The Influence of Surface Roughness on Instrumented Indentation Testing (IIT). *CSM Instruments* **2007,** *No.23*; (b) Li, M.; Chen, W. M.; Cheng, Y. T.; Cheng, C. M., Influence of contact geometry on hardness behavior in nano-indentation. *Vacuum* **2009,** *84* (2), 315-320.

6. Mahoney, E.; Holt, A.; Swain, M.; Kilpatrick, N., The hardness and modulus of elasticity of primary molar teeth: an ultra-micro-indentation study. *J. Dent.* **2000,** *28* (8), 589-594.